Ultra Slow-Roll Inflation and the non-Gaussianity Consistency Relation

Jérôme Martin [1,2],* Hayato Motohashi [2,3],† and Teruaki Suyama [2‡]
[1] *Institut d'Astrophysique de Paris, UMR 7095-CNRS, Université Pierre et Marie Curie, 98 bis boulevard Arago, 75014 Paris, France*
[2] *Research Center for the Early Universe (RESCEU), Graduate School of Science, The University of Tokyo, Tokyo 113-0033, Japan*
[3] *Department of Physics, Graduate School of Science, The University of Tokyo, Tokyo 113-0033, Japan*

Ultra slow-roll inflation has recently been used to challenge the non-Gaussianity consistency relation. We show that this inflationary scenario belongs to a one parameter class of models and we study its properties and observational predictions. We demonstrate that the power spectrum remains scale-invariant and that the bi-spectrum is of the local type with $f_{\rm NL} = 5(3 - n_{\rm S})/4$ which, indeed, represents a modification of the consistency relation. However, we also show that the system is unstable and suffers from many physical problems among which is the difficulty to correctly WMAP normalize the model. We conclude that ultra slow-roll inflation remains a very peculiar case, the physical relevance of which is probably not sufficient to call into question the validity of the consistency relation.

PACS numbers: 98.80.Cq

I. INTRODUCTION

The theory of inflation convincingly describes the physical conditions that prevailed in the very early Universe [1–5]. However, there are many models of inflation and it is not yet clear which scenario is actually realized in Nature. For this reason, the recent developments in the calculations of higher correlation functions [6] are important since they might allow us to constrain and maybe rule out many models of inflation. For instance, the simplest scenarios (*i.e.* a slowly rolling single field with a canonical kinetic term) are known to predict a negligible level of non-Gaussianity, of the order of the slow-roll parameters [7–12]. Therefore, if any non-Gaussianity is detected in the future (for instance with the Planck satellite), these models would be excluded.

Recently, however, it was argued in Ref. [13] that this is not necessarily true for the simple scenarios mentioned above. An explicit counter-example was investigated in Ref. [13] and it was shown that, in this particular case, the value of the $f_{\rm NL}$ parameter can be a few instead of being negligible. Since this result challenges a well-known and important theorem, it is important to study in more detail the model that has been utilized to obtain this conclusion. In particular, one would like to know whether this just represents a very peculiar case or whether this can correspond to a generic class of meaningful models.

In fact, the inflationary scenario used in Ref. [13] has been known for a long time and is named "ultra slow-roll" inflation. It was studied for the first time in Ref. [14] (Similar situations were also investigated in Ref. [15]). In the present article, we show that it belongs to a broader class of models that we explicitly identify. The goal of the paper is then to study this new family of scenarios, their properties and the corresponding observational predictions (power spectrum and bi-spectrum).

The paper is organized as follows. In the next section, Sec. II, we introduce ultra slow-roll inflation and show how it can be generalized. Then, we study the stability of the system and investigate whether one can easily produce 60 e-folds in the ultra slow-roll regime. Then, in Sec. III, we calculate the power spectrum of curvature fluctuations and show that it can be scale invariant even if the slow-roll parameters are not all small. In Sec. IV, we estimate the non-Gaussianities and show that the Maldacena's consistency relation is indeed violated. As a consequence the $f_{\rm NL}$ parameter is of order one in this class of models. Finally, in Sec. V, we discuss in more details the difficulties of ultra slow-roll inflation and present our conclusions.

II. ULTRA SLOW-ROLL INFLATION

Let us consider an inflationary model with a single scalar field ϕ (with a standard kinetic term). The equations of motion for ϕ and for the Friedmann-Lemaître-Robertson-Walker scale factor $a(t)$ (t denotes the cosmic time and, in the following, a dot means a derivative with respect to t) are the Friedmann and the Klein-Gordon equations, namely

$$3M_{\rm Pl}^2H^2 = \frac{\dot{\phi}^2}{2} + V(\phi), \tag{1}$$

$$\ddot{\phi} + 3H\dot{\phi} + V_\phi = 0, \tag{2}$$

where $H = \dot{a}/a$ is the Hubble parameter and $M_{\rm Pl}$ the reduced Planck mass. The background evolution can also

*E-mail:jmartin@iap.fr
†E-mail:motohashi@resceu.s.u-tokyo.ac.jp
‡E-mail:suyama@resceu.s.u-tokyo.ac.jp

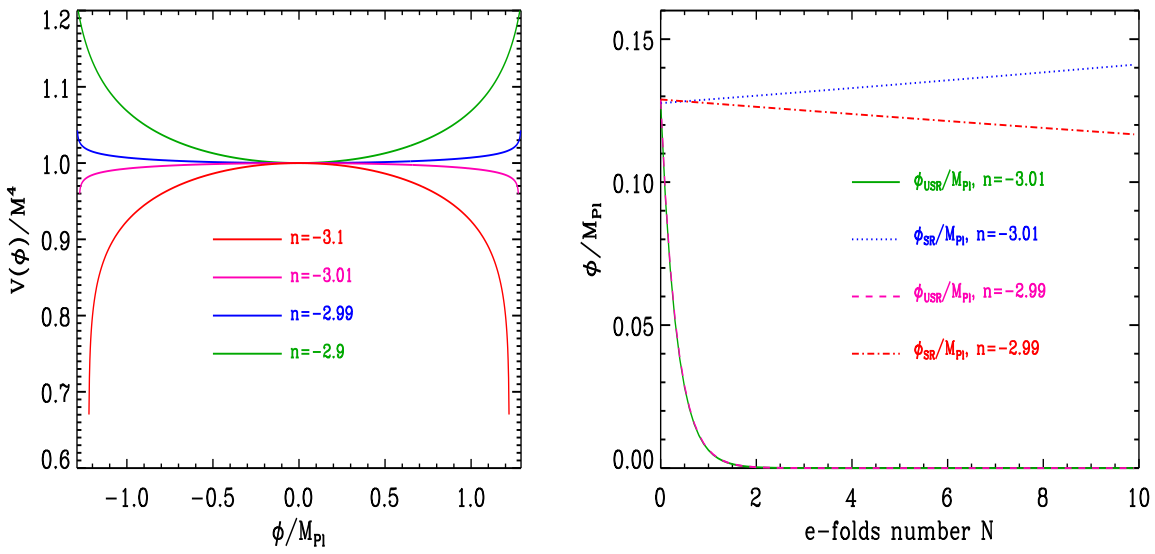

FIG. 1: Left panel: new family of ultra slow-roll potentials for different values of the parameter n. Right panel: classical ultra slow-roll and slow-roll trajectories for $n = -3.01$ (solid green line and dotted blue line) and $n = -2.99$ (dashed pink line and dotted dashed red line). The initial condition for the scalar field is chosen to be $\phi_{\rm ini} = 0.1\,\phi_{\rm lim}$.

be characterized in terms of the slow-roll parameters (or horizon-flow parameters) defined by

$$\epsilon_{i+1} = \frac{{\rm d}\ln\epsilon_i}{{\rm d}N}, \tag{3}$$

where N denotes the number of e-folds, $N \equiv \ln(a/a_{\rm ini})$ ($a_{\rm ini}$ being the scale factor at the beginning of inflation). The hierarchy starts with $\epsilon_0 \propto 1/H$ which implies that the first slow-roll parameter can be expressed as

$$\epsilon_1 \equiv -\frac{\dot{H}}{H^2} = \frac{\dot{\phi}^2}{2M_{\rm Pl}^2H^2}. \tag{4}$$

The second slow-roll parameter can be used to express the acceleration of the field, namely

$$\epsilon_2 = 2\epsilon_1 + 2\frac{\ddot{\phi}}{H\dot{\phi}}. \tag{5}$$

Inflation requires $\epsilon_1 < 1$ and the slow-roll approximation is valid if all the horizon-flow parameters are small, $\epsilon_i \ll 1$ during inflation.

As discussed in the introduction, if the potential is exactly flat, then the Klein-Gordon equation implies that $\ddot{\phi}/(H\dot{\phi}) = -3$ and this corresponds to the situation discussed in Ref. [14] and named "ultra slow-roll inflation". In this case, despite the flatness of the potential, the slow-roll parameters are not all small: usually $\epsilon_1 \ll 1$ but obviously $\epsilon_2 = \mathcal{O}(1)$. As a consequence, one could expect the power spectrum to deviate from scale-invariance but, as shown in Ref. [14], and as discussed in more detail in the next section, this is in fact not the case. This makes this model a priori interesting since this shows that scale invariance can be obtained even if the slow-roll approximation is violated. This also raises the question of whether this is peculiar to the property $V_\phi = 0$ or whether this can also be obtained in a broader context. In order to investigate this issue let us consider the more general condition

$$\ddot{\phi} = nH\dot{\phi}, \tag{6}$$

where n is now an arbitrary number, not necessarily equal to -3. Let us also assume that the first slow-roll parameter is still very small, $\epsilon_1 \ll 1$. Obviously, the case $n \simeq 0$ corresponds to slow-roll and $n = -3$ to ultra slow-roll. The corresponding equations of motion are given by

$$3M_{\rm Pl}^2H^2 \simeq V(\phi), \tag{7}$$

$$(n+3)H\dot{\phi} + V_\phi = 0. \tag{8}$$

From these equations, it is easy to check that $\dot{\phi} \propto a^n$, which implies that

$$\epsilon_1 \propto a^{2n}, \quad \epsilon_2 \simeq 2n, \quad \epsilon_3 = 0. \tag{9}$$

In particular, for $n = -3$, one recovers the well known scaling $\epsilon_1 \propto a^{-6}$, see Ref. [14].

From the two equations of motion (7) and (8), it is also straightforward to integrate the classical trajectory. One obtains

$$N(\phi) = -\frac{n+3}{3M_{\rm Pl}^2}\int_{\phi_{\rm ini}}^{\phi}\frac{V}{V_\phi}{\rm d}\phi, \tag{10}$$

where $\phi_{\rm ini}$ denotes the initial value of the inflaton. However, it is not obvious that this solution will satisfy the

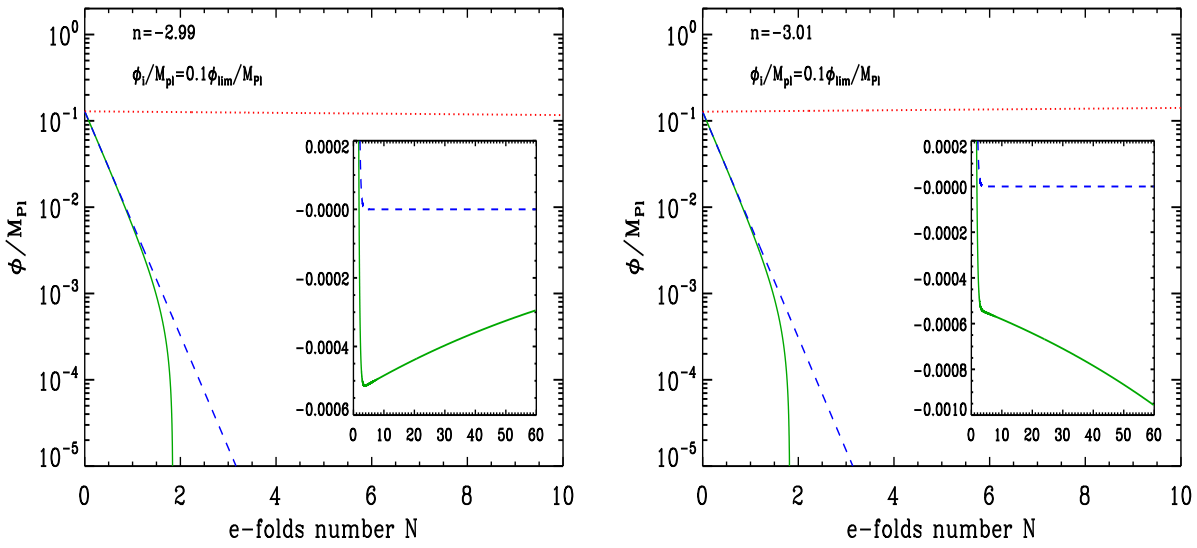

FIG. 2: Left panel: exact (numerical) evolution of the field (solid green line) compared to the ultra slow-roll solution (dashed blue line) and to the slow-roll solution (dotted red line). The parameter n is taken to be $n = -2.99$ and the initial condition is the same as in Fig. 1 (right panel), namely $\phi_{\rm ini} = 0.1\,\phi_{\rm lim}$. The inset shows the global evolution of the system on a larger time scale. Right panel: same as left panel but for $n = -3.01$.

condition (6). Requiring that this is the case, we find that the potential must obey the following differential equation

$$\frac{V_{\phi\phi}}{V} - \frac{3}{2(n+3)}\left(\frac{V_\phi}{V}\right)^2 + \frac{n(n+3)}{3M_{\rm Pl}^2} = 0. \qquad (11)$$

Interestingly enough, this differential equation can be integrated and leads to the following potential

$$V(\phi) = M^4\left[\cos\left(\sqrt{\frac{n(2n+3)}{6}}\frac{\phi-\phi_0}{M_{\rm Pl}}\right)\right]^{\frac{2(n+3)}{2n+3}}, \qquad (12)$$

where M is an arbitrary mass scale to be fixed by the Wilkinson Microwave Anisotropy Probe (WMAP) normalization and ϕ_0 an arbitrary constant that, without loss of generality, we can take to be $\phi_0 = 0$. The potentials in Eq. (12) represent a new family of model depending on one parameter, n. These potentials are represented in Fig. 1. If $n < -3$, then they are defined only in the range $-\phi_{\rm lim} < \phi < \phi_{\rm lim}$ with $\phi_{\rm lim}/M_{\rm Pl} \equiv \pi/2\sqrt{6/[n(3+2n)]}$. It is clear that if $n \simeq -3$, the potential is extremely flat, justifying the name "ultra slow-roll".

Using Eq. (10), one can compute the classical trajectory exactly. Inserting Eq. (12) into Eq. (10) leads to the following result

$$\phi_{\rm USR}(N) = M_{\rm Pl}\sqrt{\frac{6}{n(2n+3)}} \times \arcsin\left[{\rm e}^{nN}\sin\left(\sqrt{\frac{n(2n+3)}{6}}\frac{\phi_{\rm ini}}{M_{\rm Pl}}\right)\right]. \qquad (13)$$

One can check that $\phi = \phi_{\rm ini}$ implies $N = 0$. Let us notice that this expression is not well-defined for the slow-roll case $n = 0$. In this situation, one should use the following expression

$$\phi_{\rm SR}(N) = M_{\rm Pl}\sqrt{\frac{6}{n(2n+3)}} \times \arcsin\left[{\rm e}^{n(n+3)N/3}\sin\left(\sqrt{\frac{n(2n+3)}{6}}\frac{\phi_{\rm ini}}{M_{\rm Pl}}\right)\right]. \qquad (14)$$

The ultra slow-roll and slow-roll trajectories are represented in Fig. 1. The interpretation of these results can be easily understood. The slow-roll solutions just follow the curvature of the potential. Therefore, if $n \lesssim -3$ then the vacuum expectation value of the field increases (the field escapes at infinity and will meet the singularity at $\phi = \phi_{\rm lim}$) and inflation proceeds from the left to the right while, if $n \gtrsim -3$, the field value decreases toward the minimum of the potential and inflation proceeds from the right to the left. The ultra slow-roll solutions behave in a different manner. Firstly, they are very similar whatever the sign of $n+3$ provided $n \simeq -3$ and, secondly, the

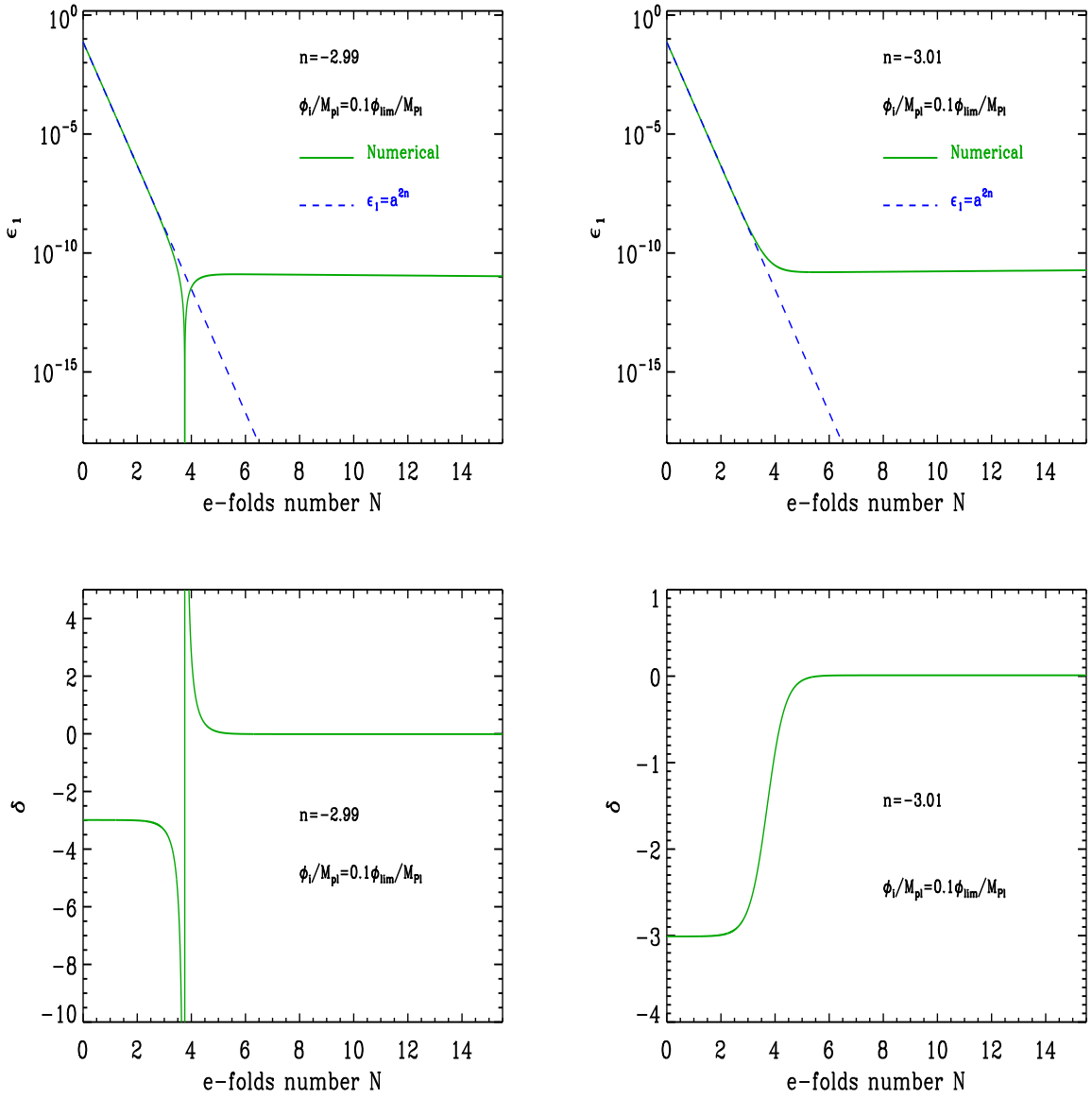

FIG. 3: Top left panel: numerical (exact) evolution of the first horizon-flow parameter ϵ_1 (solid green line) compared to its ultra-slow-roll behavior (dashed blue line) for $n = -2.99$ and $\phi_{\rm ini} = 0.1\,\phi_{\rm lim}$. Top right panel: same as top left panel but for the choice $n = -3.01$. Bottom left panel: Evolution of the quantity $\delta \equiv \ddot{\phi}/(H\dot{\phi})$ for $n = -2.99$ and $\phi_{\rm ini} = 0.1\,\phi_{\rm lim}$. Bottom right panel: same as bottom left panel but with $n = -3.01$.

field always asymptotically approaches the minimum of the potential (*i.e.* $\phi = 0$). In the case $n \lesssim -3$, this means that the field actually climbs up the potential. This is of course due to the fact that, initially, it possesses a non-vanishing and non-negligible velocity.

In order to investigate the stability of the system, we have also numerically integrated the exact equations of motion. Recall that the ultra slow-roll solution has been obtained from the exact equations of motion by neglecting the kinetic term in the right hand side of the Friedmann equation. This term, although very small, represents a perturbation for the ultra slow-roll solution. It is therefore interesting to study whether the system can stay in ultra slow-roll during a large number of e-folds. The result is presented in Fig. 2. After a few e-folds the exact solution (solid green line) leaves the ultra slow-roll solution (dashed blue line). On a larger time scale (see the insets in Fig. 2), we see that for $n \gtrsim -3$ (left panel), the field passes through the minimum, becomes negative and starts to climb up the potential in the region $\phi < 0$. Then it reaches a maximum, turns back and decreases toward the minimum. Obviously, this evolution is very

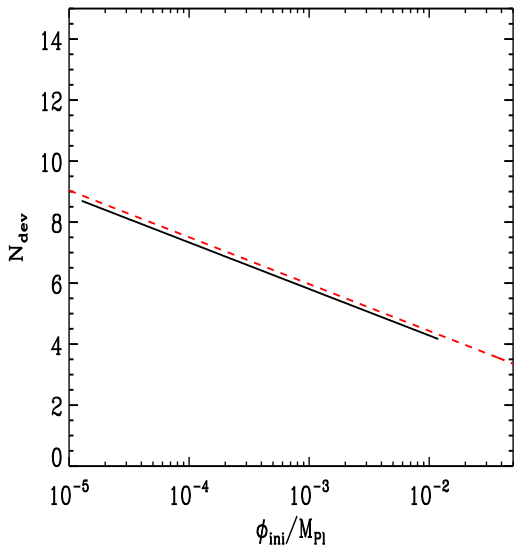

FIG. 4: Number of e-folds at which the ultra slow-roll solution is left as a function of the initial value of the field. The exact numerical result (solid black line) is in excellent agreement with the analytical estimate of Eq. (21) (dashed red curve).

different from the ultra slow-roll one. For $n \lesssim -3$ (see the right panel), the field also becomes negative but, since the curvature of the potential is now negative, it simply escapes to infinity in the region $\phi < 0$.

It is also interesting to study the behavior of the first slow-roll parameter and of $\delta \equiv \ddot{\phi}/(H\dot{\phi})$. They are represented in Fig. 3. The conclusions obtained before are confirmed. We see that ϵ_1 (top panels) scales as a^{2n} only for a few e-folds and then leaves the ultra slow-roll regime. For $n = -2.99$ (top left panel), we also notice that ϵ_1 vanishes and, of course, this corresponds to the point where, in the region $\phi < 0$, the field reaches a maximum and turns back. This is confirmed by the fact that, in the case $n = -3.01$ (top right panel), the above mentioned behavior never happens. Then, after this transitory regime, in both cases, ϵ_1 becomes constant with a very small value. The behavior of δ (bottom panels) can be understood in a similar fashion. Initially $\delta \simeq -3$ since the field starts from the ultra slow-roll regime. After a few e-folds, this solution is left and, eventually, δ reaches a regime where it remains constant with a very small value. In the case $n = -2.99$ (bottom left panel), δ diverges when $\dot{\phi} = 0$ while its evolution remains smooth if $n = -3.01$. It is clear that having ϵ_1 and δ (or, equivalently ϵ_2) small and constant corresponds to nothing but the slow-roll regime. The conclusion of our numerical investigation is therefore that the ultra slow-roll regime is unstable and is left after a few e-folds. Then, the system simply converges toward the slow-roll solution.

It is also interesting to understand when the ultra slow-roll regime is left and what are the quantities which control the instability. We now analyse this question in more detail. For this purpose let us define the following quantity

$$f \equiv \frac{\ddot{\phi}}{nH\dot{\phi}} = \frac{\delta}{n}, \tag{15}$$

which is one during ultra slow-roll inflation. Using the equations of motion, it is easy to show that it obeys the following first order non linear differential equation

$$\frac{\mathrm{d}f}{\mathrm{d}N} = -\frac{V_{\phi\phi}}{nH^2} + \frac{3\epsilon_1}{n} + f(\epsilon_1 - nf - 3) \tag{16}$$

This equation cannot be solved exactly but we can study the behavior of small perturbations. For this reason, we now define Δ by mean of the following formula $f \equiv 1+\Delta$. This quantity obeys the equation

$$\frac{\mathrm{d}\Delta}{\mathrm{d}N} = \frac{3+n}{n}\epsilon_1 - \Delta\left[3 - \epsilon_1 + n(\Delta+2)\right], \tag{17}$$

which, in the regime where $\Delta \ll 1$, can be approximated by

$$\frac{\mathrm{d}\Delta}{\mathrm{d}N} \simeq \frac{3+n}{n}\epsilon_1 - \Delta(3+2n) \tag{18}$$

Taking into account the behavior of the first slow-roll parameter during the ultra slow-roll regime, namely $\epsilon_1 = \epsilon_1|_{\mathrm{ini}} a^{2n}$, it is straightforward to obtain the following solution

$$\Delta(N) = \frac{n+3}{n(4n+3)}\epsilon_{\mathrm{ini}}\left[\mathrm{e}^{2nN} - \mathrm{e}^{-(2n+3)N}\right]. \tag{19}$$

For $|n+3| \ll 1$, one can approximate this solution by

$$\Delta(N) \simeq -\frac{n+3}{27}\epsilon_1|_{\mathrm{ini}}\mathrm{e}^{3N}. \tag{20}$$

This allows us to estimate at which e-folds, N_{dev}, the actual solution deviates from the ultra slow-roll one. Straightforward manipulations lead to

$$N_{\mathrm{dev}} \simeq \frac{2}{3}\ln\left(\frac{1}{|n|}\sqrt{\frac{54\Delta_{\mathrm{cri}}}{|n+3|}}\frac{M_{\mathrm{Pl}}}{\phi_{\mathrm{ini}}}\right), \tag{21}$$

where ϕ_{ini} is the initial value of the field and Δ_{cri} an arbitrary value at which we estimate that one has left the ultra slow-roll solution. In the following, we estimate that this is the case if the actual solution differs for more than 10% from the ultra slow-roll one, that is to say $\Delta_{\mathrm{cri}} \simeq 0.1$. We have computed this quantity numerically and have compared it with Eq. (21) in Fig. 4. Clearly the agreement is excellent. The main information brought by Eq. (21) is that the dependence in ϕ_{ini} is logarithmic. The ultra slow-roll solution is interesting if the system can follow the corresponding trajectory for at least 60 e-folds. Using Eq. (21), one can estimate what it means

for the initial conditions. Straightforward manipulations lead to the constraint

$$\frac{\phi_{\rm i}}{M_{\rm Pl}} \lesssim \frac{1}{|n|}\sqrt{\frac{54\Delta_{\rm cri}}{|n+3|}}{\rm e}^{-90}. \tag{22}$$

In other words, in order to have 60 e-folds of ultra slow-roll inflation, one must fine-tune dramatically the initial value such that it is extremely close to the top of the potential. This is of course due to the logarithmic dependence in Eq. (21) which is in fact a consequence of the instability of the system.

III. ULTRA SLOW-ROLL POWER SPECTRUM

The fact that one of the slow-roll parameters is not small immediately raises the question as to whether the model can lead to an almost scale invariant power spectrum. To address this question, it is convenient to work in terms of the so-called Mukhanov-Sasaki variable $v_{\boldsymbol{k}}$, which is related to the curvature perturbation by $\zeta_{\boldsymbol{k}} = v_{\boldsymbol{k}}/(\sqrt{2}M_{\rm Pl}a\sqrt{\epsilon_1})$. The spectrum of $\zeta_{\boldsymbol{k}}$ can be expressed as

$$\mathcal{P}_\zeta(k) \equiv \frac{k^3}{2\pi^2}\left|\zeta_{\boldsymbol{k}}\right|^2 = \frac{2k^3}{8\pi^2 M_{\rm Pl}^2}\left|\frac{v_{\boldsymbol{k}}}{a\sqrt{\epsilon_1}}\right|^2. \tag{23}$$

The variable $v_{\boldsymbol{k}}$ obeys the equation of a parametric oscillator, the time-dependent frequency being determined by the dynamics of the background [16]

$$v_{\boldsymbol{k}}'' + \left(k^2 - \frac{z''}{z}\right)v_{\boldsymbol{k}} = 0, \tag{24}$$

where the prime denotes a derivative with respect to conformal time and where z is given by $a\sqrt{\epsilon_1}$. The quantity k represents the comoving wavenumber of a Fourier mode. The "effective potential" z''/z can be expressed as

$$\frac{z''}{z} = a^2H^2\left(2-\epsilon_1+\frac{3}{2}\epsilon_2+\frac{1}{4}\epsilon_2^2-\frac{1}{2}\epsilon_1\epsilon_2+\frac{1}{2}\epsilon_2\epsilon_3\right). \tag{25}$$

Despite the appearance of the slow-roll parameters, this expression is exact. As usual, the initial conditions on the perturbations are imposed when the modes are well inside the Hubble radius during inflation. In this regime, the modes do not feel spacetime curvature and, consequently, are usually chosen to be in the Bunch-Davies vacuum. This amounts to demanding that the Mukhanov-Sasaki variable $v_{\boldsymbol{k}}$ reduces to following Minkowski-like positive frequency mode in the sub-Hubble limit:

$$\lim_{k/(a\,H)\to\infty} v_{\boldsymbol{k}} = \frac{1}{\sqrt{2\,k}}\,{\rm e}^{-i\,k\,\eta}. \tag{26}$$

In ultra slow-roll inflation, using Eq. (9), the effective potential for the perturbations can be expressed as

$$\frac{z''}{z} \simeq \frac{1}{\eta^2}\left(2+3n+n^2\right), \tag{27}$$

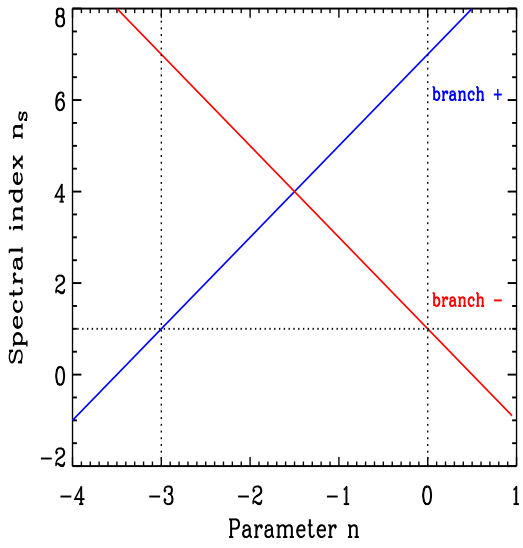

FIG. 5: Spectral index versus parameter n for the new family of potentials.

where η denotes the conformal time. We see that the solution to the mode equation can still be expressed as a Bessel function as it the case in the conventional situation. The result reads

$$v_{\boldsymbol{k}}(\eta) = -\frac{1}{2}(-\pi\eta)^{\frac{1}{2}}{\rm e}^{in\pi/2}H^{(1)}_{n+3/2}(-k\eta), \tag{28}$$

where $H^{(1)}_\nu(z)$ is the Hankel function of first type. Then, for $n < -3/2$, the power spectrum on large Hubble scales can be written as

$$\mathcal{P}_\zeta(k) = \frac{H^2}{\pi\epsilon_1 M_{\rm Pl}^2}\left(\frac{k}{aH}\right)^{2n+6}\mathcal{F}_{\rm USR}(n), \tag{29}$$

where

$$\mathcal{F}_{\rm USR}(n) \equiv \frac{2^{-2n-7}}{\Gamma^2(n+5/2)\cos^2(n\pi)}. \tag{30}$$

To our knowledge, this solution is new although the case $n = -3$ was found before in Ref. [14]. If $n > -3/2$, then one has

$$\mathcal{P}_\zeta(k) = \frac{H^2}{\pi\epsilon_1 M_{\rm Pl}^2}\left(\frac{k}{aH}\right)^{-2n}\mathcal{F}_{\rm SR}(n), \tag{31}$$

where

$$\mathcal{F}_{\rm SR}(n) \equiv \frac{2^{-1+2n}}{\Gamma^2(-n-1/2)\cos^2(n\pi)}. \tag{32}$$

Finally, it remains the case $n = -3/2$. One finds

$$\mathcal{P}_\zeta(k) = \frac{H^2}{\pi\epsilon_1 M_{\rm Pl}^2}\left(\frac{k}{aH}\right)^3\frac{1}{4\pi^2}\ln^2\left(\frac{k}{aH}\right), \tag{33}$$

In all these expressions (and this is of course crucial for the case $n < -3/2$), ϵ_1 must be evaluated not at the time of Hubble radius crossing but at the time of consideration, typically the end of inflation (of course, in the slow-roll case, this does not make a difference since the slow-roll parameters remain small and constant). The above expressions lead to the following spectral index for the power spectrum

$$n_{\rm S} - 1 = \begin{cases} 2(n+3), & n < -3/2 \\ -2n, & n > -3/2 \\ 3 + 2\ln^{-1}\left[k/(aH)\right], & n = -3/2. \end{cases}$$

The spectral index versus the parameter n is represented in Fig. 5. One sees that scale invariance is achieved for two values, namely $n \simeq 0$ which corresponds to the usual slow-roll and $n \simeq -3$ which corresponds to ultra slow-roll. If $n \lesssim -3$ the spectrum is red while if $n \gtrsim -3$, it is blue. It is easy to check that $0.96 < n_{\rm S} < 1$, see Ref. [17], corresponds to $-3.02 < n < -3$. Therefore, we obtain a new family of solutions leading to an almost scale invariant power spectrum but, clearly, n cannot deviate from -3 too strongly. One can also re-express the spectral index in terms of the slow-roll parameters. For the slow-roll regime one obtains $n_{\rm S} = 1 - \epsilon_2$ while for the ultra slow-roll regime one has

$$n_{\rm S} = 2n + 6 = 7 + \epsilon_2. \tag{34}$$

This should be compared to the standard slow-roll formula, $n_{\rm S} = 1 - 2\epsilon_1 - \epsilon_2$. Of course, in the slow-roll regime, we obtain exactly the same equation given that $\epsilon_1 \ll 1$. In the ultra slow-roll regime, however, we observe a breakdown of this result. This was already noticed in Ref. [14] for the case $n = -3$ and it was shown in that reference that this is due to a breakdown of the horizon crossing formalism. Indeed, for $n = -3$, the slow-roll formalism leads to $n_{\rm S} = 7$ instead of the correct result $n_{\rm S} = 1$.

It is also interesting to discuss in more detail the behavior of curvature perturbations on large scales. During inflation, the super-Hubble condition $k/(a\,H) \ll 1$ amounts to neglecting the k^2 term with respect to the effective potential z''/z in the differential equation (24). In such a case, it is straightforward to show that the super-Hubble solution to $v_{\boldsymbol{k}}$ can be written as follows

$$v_{\boldsymbol{k}}(\eta) \;\simeq\; A_{\boldsymbol{k}}\, z(\eta) + \, B_{\boldsymbol{k}}\, z(\eta) \int^{\eta} \frac{{\rm d}\bar{\eta}}{z^2(\bar{\eta})}, \tag{35}$$

where $A_{\boldsymbol{k}}$ and $B_{\boldsymbol{k}}$ are k-dependent constants that are determined by the Bunch-Davies initial condition (26) chosen in the sub-Hubble limit. In our case, it is easy to show that this reduces to

$$\zeta_{\boldsymbol{k}} \propto A_{\boldsymbol{k}} + B_{\boldsymbol{k}}\, a^{-(2n+3)}. \tag{36}$$

In the slow-roll regime, the first term represents the growing mode while the second one corresponds to the decaying one. In the ultra slow-roll regime however, the second term dominates over the first one (A similar situation was also studied in Refs. [18, 19]). This implies in particular that the power spectrum is still a time-dependent quantity on super-Hubble scales contrary to the standard case where it is conserved. This is apparent in Eq. (29) where the ϵ_1 term in the denominator is a time-dependent quantity. On the contrary, the same factor in Eq. (31) is constant in time and, as a consequence, the slow-roll power spectrum does not evolve on large scales. It is also worth mentioning that curvature perturbations grow on sub-Hubble scales as well. Indeed since $\zeta_{\boldsymbol{k}} \sim v_{\boldsymbol{k}}/(a\sqrt{\epsilon_1})$ and since $|v_{\boldsymbol{k}}|$ stays constant in this case, this immediately implies $|\zeta_{\boldsymbol{k}}| \propto a^{-(n+1)}$. In the slow-roll case, curvature perturbations decreases $\propto a^{-1}$.

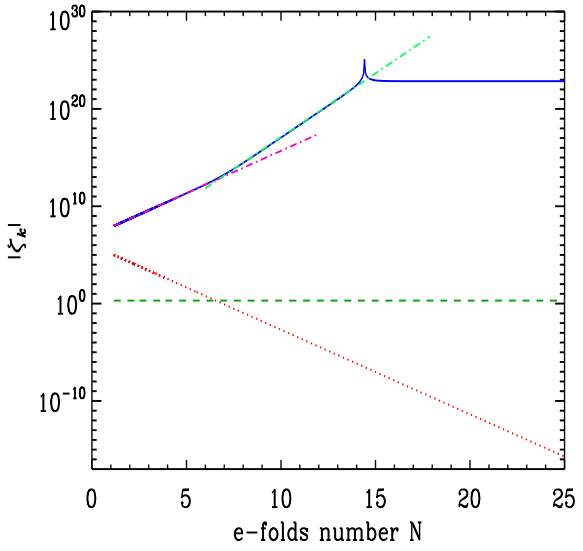

FIG. 6: Exact (numerical) evolution of curvature perturbations (solid blue line) versus the number of e-folds. The dotted dashed pink line represents the scaling $\propto a^{-(n+1)}$ while dotted dashed green line correspond to the scaling $\propto a^{-(2n+3)}$. The dotted red line is the quantity $k^2/(aH)^2$ for a mode such that $k/a_{\rm ini} \sim 50 H_{\rm ini}$ at the beginning of inflation. The dashed green line represents the quantity $\eta^2 z''/z$.

In order to check these considerations, we have numerically integrated Eq. (24). The result is presented in Fig. 6. The modulus of curvature perturbations corresponds to the solid blue line. The effective potential for the perturbations $\eta^2 z''/z$ is the dashed green line while $k^2/(a^2H^2)$ is the dotted red line. When the dotted red line is above the dashed green one, the mode is within the Hubble radius and when it is below, the mode is outside the Hubble radius. In Fig. 6, we see that the mode starts its evolution deep inside the Hubble radius and crosses it out around $N \simeq 6$. We verify that, inside the Hubble radius, $|\zeta_{\boldsymbol{k}}|$ grows like $a^{-(n+1)}$, this particular scaling being represented by the dotted-dashed pink line. When the mode crosses out the Hubble radius, it is apparent that the behavior of $|\zeta_{\boldsymbol{k}}|$ is modified. The dotted dashed

green line represents the scaling $a^{-(2n+3)}$ and one sees in the figure that it is indeed the scaling of $|\zeta_{\boldsymbol{k}}|$. Therefore, our numerical integration confirms that, in ultra slow-roll inflation, curvature perturbations grow on small and large scales. Around $N \simeq 13$, ultra slow-roll inflation comes to an end and, as a consequence, the growth of $\zeta_{\boldsymbol{k}}$ stops. Then, as clearly seen in the figure, $\zeta_{\boldsymbol{k}}$ stays constant as usual in the slow-roll regime on large scales.

This continuous growth of curvature perturbations during ultra slow-roll inflation turns out to have important physical implications. Since $\mathcal{P}_{\zeta}(k)$ is a time-dependent quantity even on large scales, this means that the amplitude of the power spectrum at the time when inflation ends must now be compared with the WMAP normalization (in the slow-roll case, it is sufficient to normalize the power spectrum when the modes of cosmological interest today leaves the Hubble radius during inflation). If $n \simeq -3$, the power spectrum of the curvature perturbation at the time when inflation ends is given by

$$\mathcal{P}_{\zeta} = \frac{1}{24\pi^2\epsilon_{1*}} e^{6\Delta N_*} \biggl(\frac{M}{M_{\rm Pl}}\biggr)^4, \tag{37}$$

where $\Delta N_* \simeq 50 - 60$ is the number of e-fold between the Hubble radius crossing time of the relevant mode and the end of inflation. The quantity ϵ_{1*} is ϵ_1 evaluated at the Hubble radius crossing time. From the WMAP normalization $\mathcal{P}_{\zeta} = 2.4 \times 10^{-9}$, see Ref. [17], we find that for $\Delta N_* = 60$, M must satisfy

$$\frac{M}{M_{\rm Pl}} = 7 \times 10^{-42} \biggl(\frac{\epsilon_{1*}}{0.01}\biggr)^{1/4}, \tag{38}$$

which is far below the Big Bang Nucleosynthesis (BBN) bound $M > \mathcal{O}(\mathrm{MeV})$. The result is expected. The quantity $|\zeta_{\boldsymbol{k}}|$ grows so much during ultra slow-roll inflation that, in order to match the correct level of Cosmic Microwave Background (CMB) fluctuations, one must compensate by a tiny mass scale in the potential. Let us notice that we also implicitly assume that, after inflation, the growth of $|\zeta_{\boldsymbol{k}}|$ stops. In addition, the above estimate is very conservative because it is expressed in terms of ϵ_{1*}. Since ϵ_1 is decreasing from the beginning of inflation, it is likely that $\epsilon_{1*} \ll 1$. In other words, instead of ΔN_*, the constraint could also be written in terms of the total number of e-folds. This means that a physically relevant ultra slow-roll inflation model can last only for a much shorter period than the 60 e-folds usually required.

IV. ULTRA SLOW-ROLL NON GAUSSIANITY

Let us now turn to the calculation of the three-point correlation function. For the case $n = -3$, the calculation was done for the first time in Ref. [13]. Here we generalize this result for an arbitrary value of the parameter n. As is well-known, for slow-roll single field inflation with a standard kinetic term, the level of non-Gaussianity is very small, of the order of the slow-roll parameters, see Refs. [7–12]. This result is still true for ultra slow-roll inflation but, now, one of the slow-roll parameters is of order one. Therefore, one expects a $f_{\rm NL}$ parameter of order one as well. We will see that this is what happened although, as noticed in Ref. [13], the relation between $f_{\rm NL}$ and $n_{\rm S}$ is modified.

The scalar bi-spectrum $\mathcal{B}_{\rm S}(\boldsymbol{k}_1, \boldsymbol{k}_2, \boldsymbol{k}_3)$ is defined in terms of the three point correlation functions of the Fourier modes of the curvature perturbation ζ as follows [17, 20]:

$$\langle \hat{\zeta}_{\boldsymbol{k}_1}\, \hat{\zeta}_{\boldsymbol{k}_2}\, \hat{\zeta}_{\boldsymbol{k}_3} \rangle = (2\,\pi)^3\, \mathcal{B}_{\rm S}(\boldsymbol{k}_1, \boldsymbol{k}_2, \boldsymbol{k}_3) \times \delta^{(3)}\left(\boldsymbol{k}_1 + \boldsymbol{k}_2 + \boldsymbol{k}_3\right). \tag{39}$$

For convenience, we shall set $G(\boldsymbol{k}_1, \boldsymbol{k}_2, \boldsymbol{k}_3) = (2\,\pi)^{9/2}\, \mathcal{B}_{\rm S}(\boldsymbol{k}_1, \boldsymbol{k}_2, \boldsymbol{k}_3)$. Using the Maldacena formalism [6], the quantity $G(\boldsymbol{k}_1, \boldsymbol{k}_2, \boldsymbol{k}_3)$ can be expressed as [21–23] (recall that the function $f_{\boldsymbol{k}}$ below is the mode function that appears in front of the annihilation and creation operators in the canonical decomposition of the operator $\hat{\zeta}$)

$$\begin{aligned} G(\boldsymbol{k}_1, \boldsymbol{k}_2, \boldsymbol{k}_3) &\equiv \sum_{C=1}^{7} G_{_C}(\boldsymbol{k}_1, \boldsymbol{k}_2, \boldsymbol{k}_3) \\ &\equiv M_{\rm Pl}^2 \sum_{C=1}^{6} \biggl[f_{\boldsymbol{k}_1}(\eta_{\rm f})\, f_{\boldsymbol{k}_2}(\eta_{\rm f})\, f_{\boldsymbol{k}_3}(\eta_{\rm f}) \mathcal{G}_{_C}(\boldsymbol{k}_1, \boldsymbol{k}_2, \boldsymbol{k}_3) + f^*_{\boldsymbol{k}_1}(\eta_{\rm f})\, f^*_{\boldsymbol{k}_2}(\eta_{\rm f})\, f^*_{\boldsymbol{k}_3}(\eta_{\rm f})\, \mathcal{G}^*_{_C}(\boldsymbol{k}_1, \boldsymbol{k}_2, \boldsymbol{k}_3) \biggr] \\ &\quad + G_7(\boldsymbol{k}_1, \boldsymbol{k}_2, \boldsymbol{k}_3), \end{aligned} \tag{40}$$

where $\eta_{\rm f}$ denotes the final time when the bi-spectrum is to be evaluated. The quantities $\mathcal{G}_{_C}(\boldsymbol{k}_1, \boldsymbol{k}_2, \boldsymbol{k}_3)$ with $C =$

$1, \cdots, 6$ are described by the integrals [21–23]

$$\mathcal{G}_1(\boldsymbol{k}_1,\boldsymbol{k}_2,\boldsymbol{k}_3) = 2\,i\int_{\eta_\mathrm{i}}^{\eta_\mathrm{f}}\mathrm{d}\eta\,a^2\,\epsilon_1^2\,\big(f^*_{\boldsymbol{k}_1}\,f'^*_{\boldsymbol{k}_2}\,f'^*_{\boldsymbol{k}_3}+\text{two permutations}\big), \tag{41}$$

$$\mathcal{G}_2(\boldsymbol{k}_1,\boldsymbol{k}_2,\boldsymbol{k}_3) = -2\,i\,\left(\boldsymbol{k}_1\cdot\boldsymbol{k}_2+\text{two permutations}\right)\int_{\eta_\mathrm{i}}^{\eta_\mathrm{f}}\mathrm{d}\eta\,a^2\,\epsilon_1^2\,f^*_{\boldsymbol{k}_1}\,f^*_{\boldsymbol{k}_2}\,f^*_{\boldsymbol{k}_3}, \tag{42}$$

$$\mathcal{G}_3(\boldsymbol{k}_1,\boldsymbol{k}_2,\boldsymbol{k}_3) = -2\,i\int_{\eta_\mathrm{i}}^{\eta_\mathrm{f}}\mathrm{d}\eta\,a^2\,\epsilon_1^2\left[\left(\frac{\boldsymbol{k}_1\cdot\boldsymbol{k}_2}{\boldsymbol{k}_2^2}\right)\,f^*_{\boldsymbol{k}_1}\,f'^*_{\boldsymbol{k}_2}\,f'^*_{\boldsymbol{k}_3}+\text{five permutations}\right], \tag{43}$$

$$\mathcal{G}_4(\boldsymbol{k}_1,\boldsymbol{k}_2,\boldsymbol{k}_3) = i\int_{\eta_\mathrm{i}}^{\eta_\mathrm{f}}\mathrm{d}\eta\,a^2\,\epsilon_1\,\epsilon_2'\,\big(f^*_{\boldsymbol{k}_1}\,f^*_{\boldsymbol{k}_2}\,f'^*_{\boldsymbol{k}_3}+\text{two permutations}\big), \tag{44}$$

$$\mathcal{G}_5(\boldsymbol{k}_1,\boldsymbol{k}_2,\boldsymbol{k}_3) = \frac{i}{2}\int_{\eta_\mathrm{i}}^{\eta_\mathrm{f}}\mathrm{d}\eta\,a^2\,\epsilon_1^3\left[\left(\frac{\boldsymbol{k}_1\cdot\boldsymbol{k}_2}{\boldsymbol{k}_2^2}\right)\,f^*_{\boldsymbol{k}_1}\,f'^*_{\boldsymbol{k}_2}\,f'^*_{\boldsymbol{k}_3}+\text{five permutations}\right], \tag{45}$$

$$\mathcal{G}_6(\boldsymbol{k}_1,\boldsymbol{k}_2,\boldsymbol{k}_3) = \frac{i}{2}\int_{\eta_\mathrm{i}}^{\eta_\mathrm{f}}\mathrm{d}\eta\,a^2\,\epsilon_1^3\left\{\left[\frac{\boldsymbol{k}_1^2\,(\boldsymbol{k}_2\cdot\boldsymbol{k}_3)}{\boldsymbol{k}_2^2\,\boldsymbol{k}_3^2}\right]\,f^*_{\boldsymbol{k}_1}\,f'^*_{\boldsymbol{k}_2}\,f'^*_{\boldsymbol{k}_3}+\text{two permutations}\right\}, \tag{46}$$

where η_i denotes the time when the modes $f_{\boldsymbol{k}}$ are well inside the Hubble radius during inflation. The additional, seventh term $G_7(\boldsymbol{k}_1,\boldsymbol{k}_2,\boldsymbol{k}_3)$ arises due to a field redefinition, and its contribution to $G(\boldsymbol{k}_1,\boldsymbol{k}_2,\boldsymbol{k}_3)$ is found to be

$$G_7(\boldsymbol{k}_1,\boldsymbol{k}_2,\boldsymbol{k}_3) = \left[\frac{\epsilon_2}{2}-2(2n+3)\right]\left[|f_{\boldsymbol{k}_2}(\eta_\mathrm{f})|^2\,|f_{\boldsymbol{k}_3}(\eta_\mathrm{f})|^2+\text{two permutations}\right]. \tag{47}$$

In the ultra slow-roll case, since ϵ_1 is very tiny while $\epsilon_2=\mathcal{O}(1)$, the above equations show that G_7 gives the dominant contribution to the bi-spectrum for any configuration of the triangle formed by the vectors $\boldsymbol{k}_1$, $\boldsymbol{k}_2$ and $\boldsymbol{k}_3$. Notice that the second term $-2(2n+3)$ in Eq. (47) is absent in the standard slow-roll case. This originates from the fact that the terms in the cubic action that must be removed by field redefinition are of the form $a\epsilon_2\zeta^2/2+2\zeta\zeta'/H+\cdots$, where the dots denote terms that always involve a spatial derivative of the curvature perturbation. In the standard case, only the first term is important because of the conservation of curvature perturbations on super-Hubble scales. On the other hand, in the present case where the decaying mode dominates over the growing mode, the second term also contributes since $\zeta'\neq 0$ [13]. It is actually this second term that leads to the violation of the standard non-Gaussianity consistency relation. Then, the bi-spectrum becomes

$$\mathcal{B}_\mathrm{S}(\boldsymbol{k}_1,\boldsymbol{k}_2,\boldsymbol{k}_3) = -\frac{3}{4}\,(n+2)\,\frac{(2\pi)^{-1/2}}{k_1^3k_2^3k_3^3}\times\left[k_3^3P_\zeta(k_1)P_\zeta(k_2)+2\text{ perms}\right] \tag{48}$$

Interestingly enough, the bi-spectrum is of the local type not only in the squeezed limit but also for any other set of $(\boldsymbol{k}_1,\boldsymbol{k}_2,\boldsymbol{k}_3)$. Then, from the above expression, we can immediately read f_NL which is given by[1]

$$f_\mathrm{NL}^\mathrm{USR} = -\frac{5}{2}(n+2). \tag{49}$$

As noticed in Ref. [13], this gives a relation between f_NL and n different from the Maldacena consistency relation which yields $f_\mathrm{NL}^\mathrm{sq}=5(1-n_\mathrm{S})/12\simeq 5n/6$. Finally, it is also interesting to provide a relation between f_NL and n_S:

$$f_\mathrm{NL}^\mathrm{USR} = \frac{5}{4}\,(3-n_\mathrm{S})\,, \tag{50}$$

where we emphasized again the fact that it is valid for any configuration, not only in the squeezed limit. This clearly shows that f_NL becomes of order one even if the power-spectrum is almost scale invariant. Such a signal would be marginally detectable by the Planck satellite which, in principle, can see $|f_\mathrm{NL}|\gtrsim 5$. Finally, let also mention that, in order for the bi-spectrum we have just calculated to describe the non-Gaussianity which would actually be observed in the sky, it is necessary to assume that the growth of $\zeta_{\boldsymbol{k}}$ stops after the end of inflation and that reheating will not modify the result. The latter seems very reasonable as recently shown in Ref. [26].

V. DISCUSSION AND CONCLUSIONS

Let us now recap our main results. Ultra slow-roll is not new and was studied in Ref. [14]. It is characterized by a situation where the first horizon flow parameter is very small but the second one is of order one. In this paper, we have generalized the ultra slow-roll regime to

[1] We use the same f_NL as the one used by WMAP. Notice that Refs. [6, 22, 24, 25] use a different sign convention.

a one parameter family models. We have seen that, in ultra slow-roll inflation, the curvature perturbation can be dominated by the decaying mode. Despite this property, the corresponding power spectrum remains scale invariant and, hence, in agreement with the CMB observations. This leads to the interesting situation where $f_{\rm NL}$ is of order one even in a single field model with a standard kinetic term. This clearly violates the Maldacena consistency relation.

However, ultra slow-roll inflation appears to be plagued with many difficulties. Firstly, the system is unstable and the ultra slow roll solution is left after a few e-folds only unless one artificially fine tunes the initial conditions. Secondly, the continuous growth of curvature perturbations implies that the mass scale of the potential must be extremely small in order to match the observed level of CMB anisotropy. In fact the corresponding value of M turns out to be unphysical. There is also a third difficulty that we now discuss. As is well-known, when the potential is very flat, the quantum effects can dominate over the classical dynamics. In ultra slow-roll inflation, the typical variation of the scalar field (during one e-fold) due to the classical dynamics can be expressed as

$$\Delta\phi_{\rm cl} \simeq \frac{-3M_{\rm Pl}^2}{3+n}\frac{V_\phi}{V}. \tag{51}$$

On the other hand, typical quantum jumps are given by $\Delta\phi_{\rm quant} \simeq H/(2\pi)$. Therefore, the classical equations of motion are valid only if $\Delta\phi_{\rm cl} \gg \Delta\phi_{\rm quant}$. Using the previous considerations, this leads to

$$\frac{\phi}{M_{\rm Pl}} \gg \frac{M^2}{2\pi|n|\sqrt{3}M_{\rm Pl}^2}. \tag{52}$$

Given the requirement (22), one can have 60 e-folds of ultra slow-roll inflation in the classical regime only if

$$\frac{M^2}{2\pi|n|\sqrt{3}M_{\rm Pl}^2} < \frac{1}{|n|}\sqrt{\frac{54\Delta_{\rm cri}}{|n+3|}}{\rm e}^{-90}, \tag{53}$$

that is to say

$$\frac{M}{M_{\rm Pl}} \lesssim \left(\frac{648\pi^2\Delta_{\rm cri}}{|n+3|}\right)^{1/4}{\rm e}^{-45}. \tag{54}$$

For $\Delta_{\rm cri} = 0.1$ and $|n+3| = 0.01$, this gives

$$M \lesssim 1.1\,{\rm GeV}. \tag{55}$$

This is larger than the BBN bound $M > \mathcal{O}({\rm MeV})$ but remains rather small. As we have seen the WMAP normalization provides a much tighter constraint on M. Nevertheless, it is likely that in a realistic realization of ultra slow-roll inflation the quantum effects play a dominant role.

It seems therefore difficult to produce 60 e-folds of inflation in the ultra slow-roll regime. One can wonder whether the very flat region of the potential could only represents a limited part of the full potential. It seems however difficult to understand how the field could enter this part of the potential with the correct initial conditions $\ddot{\phi} = nH\dot{\phi}$. Of course if $V_\phi = 0$ exactly, then the previous condition is true but this does not represents a realistic case as there will always be corrections, even if extremely small. In this case, moreover, the dynamics would be completely controlled by quantum effects.

In conclusion, ultra slow-roll inflation represents an interesting playground but it remains a challenge to build a physically relevant model that would exhibit in this regime. In fact, this shows how robust the Maldacena consistency condition is. In order to violate it, we are forced to consider situations that appear to be plagued with many physical difficulties.

Acknowledgments

This work was supported by JSPS Research Fellowships for Young Scientists (H.M.) and Grant-in-Aid for JSPS Fellows No. 1008477 (T.S.). J.M. would like to thank RESCEU (University of Tokyo) for warm hospitality. We would like to thank J. Yokoyama for careful reading of the manuscript and interesting comments.

[1] J. Martin and C. Ringeval, JCAP **0608**, 009 (2006), astro-ph/0605367.
[2] L. Lorenz, J. Martin, and C. Ringeval, JCAP **0804**, 001 (2008), 0709.3758.
[3] L. Lorenz, J. Martin, and C. Ringeval, Phys.Rev. **D78**, 063543 (2008), 0807.2414.
[4] J. Martin and C. Ringeval, Phys.Rev. **D82**, 023511 (2010), 1004.5525.
[5] J. Martin, C. Ringeval, and R. Trotta, Phys.Rev. **D83**, 063524 (2011), 1009.4157.
[6] J. M. Maldacena, JHEP **0305**, 013 (2003), astro-ph/0210603.
[7] A. Gangui, F. Lucchin, S. Matarrese, and S. Mollerach, Astrophys.J. **430**, 447 (1994), astro-ph/9312033.
[8] A. Gangui, Phys.Rev. **D50**, 3684 (1994), astro-ph/9406014.
[9] L.-M. Wang and M. Kamionkowski, Phys.Rev. **D61**, 063504 (2000), astro-ph/9907431.
[10] A. Gangui and J. Martin, Mon.Not.Roy.Astron.Soc. (1999), astro-ph/9908009.
[11] A. Gangui and J. Martin, Phys.Rev. **D62**, 103004 (2000), astro-ph/0001361.

[12] A. Gangui, J. Martin, and M. Sakellariadou, Phys.Rev. **D66**, 083502 (2002), astro-ph/0205202.
[13] M. H. Namjoo, H. Firouzjahi, and M. Sasaki (2012), 1210.3692.
[14] W. H. Kinney, Phys.Rev. **D72**, 023515 (2005), gr-qc/0503017.
[15] S. Inoue and J. Yokoyama, Phys.Lett. **B524**, 15 (2002), hep-ph/0104083.
[16] V. F. Mukhanov, H. Feldman, and R. H. Brandenberger, Phys.Rept. **215**, 203 (1992).
[17] E. Komatsu et al. (WMAP Collaboration), Astrophys.J.Suppl. **192**, 18 (2011), 1001.4538.
[18] O. Seto, J. Yokoyama, and H. Kodama, Phys.Rev. **D61**, 103504 (2000), astro-ph/9911119.
[19] R. Saito, J. Yokoyama, and R. Nagata, JCAP **0806**, 024 (2008), 0804.3470.
[20] D. Larson, J. Dunkley, G. Hinshaw, E. Komatsu, M. Nolta, et al., Astrophys.J.Suppl. **192**, 16 (2011), 1001.4635.
[21] D. Seery and J. E. Lidsey, JCAP **0506**, 003 (2005), astro-ph/0503692.
[22] X. Chen, Phys.Rev. **D72**, 123518 (2005), astro-ph/0507053.
[23] X. Chen, Adv.Astron. **2010**, 638979 (2010), 1002.1416.
[24] J. Martin and L. Sriramkumar, JCAP **1201**, 008 (2012), 1109.5838.
[25] D. K. Hazra, L. Sriramkumar, and J. Martin (2012), 1201.0926.
[26] D. K. Hazra, J. Martin, and L. Sriramkumar, Phys.Rev. **D86**, 063523 (2012), 1206.0442.